Outdoor Characterization of Solar Cells With Microstructured Antireflective Coating in a Concentrator Photovoltaic Monomodule

Arnaud Joel Kinfack Leoga, Arnaud Ritou, Mathieu Blanchard, Lysandre Dirand, Yanis Prunier, Philippe St-Pierre, David Chuet, Philippe-Olivier Provost, Maïté Volatier, Vincent Aimez, *Member, IEEE*, Gwenaëlle Hamon, *Member, IEEE*, Abdelatif Jaouad, Christian Dubuc, and Maxime Darnon

***Abstract*—Microstructured antireflective coatings (ARCs) have been identified as a promising solution to reduce optical losses in concentrator photovoltaics' (CPV) modules. We fabricated and tested in field a CPV module made of four monomodules with a concentration factor of 250× that embed either solar cells with microstructured encapsulating ARC or solar cells with multilayer ARC as a reference. The microstructured encapsulating ARC was made of semiburied silica beads in polydimethylsiloxane. The module was in operation for one year in the severe climatic conditions of Sherbrooke, QC, Canada, before extracting the monomodules performance. Despite a suboptimal module design, we report a monomodule efficiency of 29.7% at 900 W/m^2 for a cell with microstructured encapsulating ARC. This proves the potential of microstructured encapsulating ARC to enable high-performance CPV systems.**

***Index Terms*—Antireflective coating (ARC), concentrator photovoltaics (CPV), outdoor characterization.**

Manuscript received 19 June 2023; accepted 11 July 2023. Date of publication 8 August 2023; date of current version 6 September 2023. This work was supported in part by STACE, in part by MITACS, and in part by Quebec Ministère de l'Économie et de l'Innovation. LN2 is a joint International Research Laboratory (IRL 3463) funded and co-operated in Canada by Université de Sherbrooke (UdeS) and in France by CNRS as well as ECL, INSA Lyon, and Université Grenoble Alpes (UGA). It is also supported by the Fonds de Recherche du Québec Nature et Technologie (FRQNT). *(Corresponding author: Maxime Darnon.)*

Arnaud Joel Kinfack Leoga, Mathieu Blanchard, Lysandre Dirand, Yanis Prunier, Philippe St-Pierre, David Chuet, Philippe-Olivier Provost, Maïté Volatier, Vincent Aimez, Gwenaëlle Hamon, Abdelatif Jaouad, and Maxime Darnon are with the Institut Interdisciplinaire d'Innovation Technologique (3IT), Université de Sherbrooke, Sherbrooke, QC J1K 0A5, Canada, and also with the Laboratoire Nanotechnologies Nanosystèmes (LN2) - CNRS IRL-3463, Institut Interdisciplinaire d'Innovation Technologique (3IT), Université de Sherbrooke, Sherbrooke, QC J1K 0A5, Canada (e-mail: arnaud.joel.kinfack.leoga@usherbrooke.ca; mathieu.blanchard2@usherbrooke.ca; lysandre.dirand@usherbrooke.ca; yanis.prunier@usherbrooke.ca; philippe.st-pierre3@usherbrooke.ca; david.chuet@usherbrooke.ca; philippe-olivier.provost@usherbrooke.ca; maite.volatier@usherbrooke.ca; vincent.aimez@usherbrooke.ca; gwenaelle.hamon@usherbrooke.ca; abdelatif.jaouad@usherbrooke.ca; maxime.darnon@usherbrooke.ca).

Arnaud Ritou is with the Institut Interdisciplinaire d'Innovation Technologique (3IT), Université de Sherbrooke, Sherbrooke, QC J1K 0A5, Canada, also with the Laboratoire Nanotechnologies Nanosystèmes (LN2) - CNRS IRL-3463, Institut Interdisciplinaire d'Innovation Technologique (3IT), Université de Sherbrooke, Sherbrooke, QC J1K 0A5, Canada, and also with the Saint-Augustin Canada Electric Inc., Saint-Augustin, QC G3A 1S5, Canada (e-mail: arnaud.ritou@usherbrooke.ca).

Christian Dubuc is with the Saint-Augustin Canada Electric Inc., Saint-Augustin, QC G3A 1S5, Canada (e-mail: christian.dubuc@stacelectric.com).

Color versions of one or more figures in this article are available at https://doi.org/10.1109/JPHOTOV.2023.3295498.

Digital Object Identifier 10.1109/JPHOTOV.2023.3295498

I. Introduction

CONCENTRATOR photovoltaics (CPV) is the photovoltaic technology with the highest conversion efficiency at the system level. It relies on multijunction solar cells that were originally developed for space application. To mitigate the high cost of multijunction solar cells, CPV uses optical elements (mirrors or lenses) to collect the sunlight and concentrate it onto a smaller area solar cell [1]. Current commercial CPV technologies reach more than 30% conversion efficiency at the system level, thanks to a few mm^2 solar cells and Fresnel lenses with an optical concentration of typically 500× [2]. Because of the presence of multiple optical interfaces, optical efficiency losses due to reflection cannot be neglected. To reduce reflective losses at the surface of the triple junction solar cells, interferometric multilayer antireflective coatings (ARCs), such as TiO_2/AlO_x [3] or SiN/SiO_2 [4], are deposited on the surface of the solar cells, with controlled thickness and optical index. These layers can eventually play the role of encapsulating layers to prevent the interaction of the cell with moisture and improve the system's reliability. However, such an interferometric approach is designed for normal incidence and is less effective when sunlight reaches the cell surface with an angular distribution, especially when angles are larger than 45° [5], as it is the case in some CPV systems. An alternative approach consists in micro/nanostructuring the ARC to provide a graded optical index on the cell [6], [7]. Using indoor characterizations, we have shown that the short-circuit current produced by an InGaP/InGaAs/Ge solar cell can be improved by 2.6% ± 1%, by using 1-μm-diameter silica beads embedded into a polydimethylsiloxane (PDMS) layer—the so-called microbeads ARC [8], in comparison with an $AlO_x/TiO_x/SiO_2$ encapsulating ARC.

We propose here to evaluate microbeads ARC in real operating conditions. We built a dedicated CPV module with four 250× spherical lenses [9]. Two solar cells with microbeads ARC fabricated using the process described in [8] and two reference solar cells with $AlO_x/TiO_x/SiO_2$ encapsulating ARC are integrated into the module. Each cell is independently characterized. The module has been installed for one year on an experimental sun tracker and exposed to harsh operating conditions in the solar park of Université de Sherbrooke, Sherbrooke, QC, Canada (including −30 °C nights during winter and +30 °C during summer).

II. Experimental Sections

A. Solar Cells

The solar cells are commercial triple junction solar cells from AZUR SPACE with an efficiency rated at 37.8% at 1000× (AM1.5D – 1000 W/m^2). The top electrode design was optimized for operation under 500× concentration. The solar cells are hexagonal with an active area (excluding busbars) of 6.55 mm^2. The cells are coated with a bilayer AlO_x/TiO_x ARC optimized for minimizing reflection when used with an SiO_2 encapsulating layer. Two kinds of encapsulating layers are considered. As a reference, a 100 ± 30-nm-thick layer of SiO_2 is deposited by atmospheric plasma-enhanced chemical vapor deposition. The reference cells are bonded with a conductive epoxy onto an aluminum plate, and the front electrical contact is connected by gold wirebonding. This reference corresponds to encapsulation and assembly from commercial products. The second kind of encapsulating layer (microbeads) is made of 1-μm-diameter silica beads semiburied into a 6 ± 0.2-μm-thick PDMS layer (Sylgard 184). Details on the fabrication methods and indoor characteristics of these cells are described in [8]. These cells with microbeads are mounted on an aluminum core printed circuit board and the front contact is connected by gold wirebonding.

B. Test Module and Tracker

The test module is made of two thick aluminum plates—one to support the lenses and one to support the cells—separated by aluminum posts. The lenses are plano-convex BK7 lenses from Thorlabs (LA1145) [10] glued using PDMS. They have a focal distance of 74.8 mm, a diameter of 2 in, and a clear aperture of 16.42 cm^2. The lens is not coated by an ARC. Considering the active area of the solar cells, the optical concentration of the module is 250×. The cells on the receiver are fixed onto micrometric plates for fine tuning the cell-to-lens alignment. Each cell is individually connected to the electrical characterization setup. The module is made of four lens–cell couples, referred to as monomodules in the following. Two monomodules (A and B) embed solar cells with microbeads, while two other monomodules (C and D) embed reference cells. Once the test module is mounted onto the tracker, iterative corrections of the cell's positions combined with short-circuit current measurements are performed to maximize the short-circuit current of each monomodule, and therefore optimize the cell-to-lens alignment. Afterward, the module is closed and kept water tight during operation. Fig. 1 shows pictures of the 250× module.

The test module is installed onto a STR-22G tracker from EKO [11]. This tracker has a tracking accuracy of ±0.01°. For the first year of operation, the tracker was operating in astronomical mode (open-loop tracking). However, this tracking mode induces tracking errors that depend on the hour and day of operation. To minimize the tracking errors, we implemented a new tracking algorithm called maximum current tracking (MCT). It consists in measuring the short-circuit current in 16 positions (4 × 4 resolution) of 2.25° range in azimuth and elevation centered on the astronomical position of the sun. From these measurements, we interpolate up to 100 positions (10 × 10 resolution)—this short-circuit current map yielding the maximum short-circuit current and the associated best position. While the sky is cloudless for a long enough period of time, the tracker then moves to this exact position before data acquisition. This tracking procedure is repeated for each monomodule before each measurement. Since the tracking procedure takes around 10 s per monomodule, we consider the offset between the astronomical sun's position and its real position to be constant over the 10 s alignment and measurement time.

Fig. 1. Pictures of the module installed on the EKO tracker.

Based on the cell alignment procedure and the MCT tracking algorithm, we can assume a perfect alignment of the cell, the lens, and the sun.

C. Instrumentation

The electrical characterization of the monomodules is performed using a 2601B source monitor unit (SMU) and a 3706 A multiplexer from Keithley. Between each measurement, the solar cells are maintained in an open circuit since the experimental setup does not enable continuous polarization of each individual cell. The SMU, the multiplexer, and the tracker are driven using a Raspberry Pi with dedicated controlling software written in Python. A Razon+ weather station from Kipp'n Zonen installed ∼200 m away from the test site is used to provide meteorological data (i.e., direct normal irradiance (DNI) and temperature).

D. Methodology

For all characterizations, we adhered to the recommendations from Muller [12] for data filtering for characterization under standard conditions: ambient temperature between 10 and 30 °C, DNI larger than 750 W/m^2, diffuse irradiance below 140 W/m^2, DNI deviation lower than 2% within 5 min, wind speed lower than 5 m/s, and air mass below 2. However, due to the limitations

TABLE I
CHARACTERISTICS OF CPV MONOMODULES OBTAINED FROM THE CHARACTERIZATIONS CARRIED FROM MID-AUGUST TO MID-SEPTEMBER, 2022

Monomodule	Type	J_{SC} (mA/cm²) from EQE @Cell level @AM1.5D	I_{SC} (mA) @Module level @900 W·m⁻²	Effective concentration	Short circuit current CTM	Pmax (mW) @Module level @900 W·m^{-2}	Efficiency (%)
A	Microbeads	13.24	196	226	90	439	29.7
B	Microbeads	13.20	192	222	89	425	28.8
C	Reference	12.87	172	204	82	369	25
D	Reference	12.75	144	172	69	217	14.7

of our experimental setup, specifically the unavailability of spectral content, we were unable to apply filters for precipitable water vapor or correct for cell or lens temperature. These recommendations aim to bring us as close as possible to concentrator standard operating conditions considering the constraints of our experimental setup.

To determine the *I–V* characteristics of each monomodule, the open-circuit voltage (V_{OC}) is measured first. Then, we sweep the cell voltage between 0 V and V_{OC}. Eight points are linearly measured between 0 V and 70% of V_{OC}, then 16 points are measured between 70% and 95% of V_{OC}, and 8 points between 95% of V_{OC} and V_{OC}. Since it takes around 10 s per cell for tracker positioning and cell characterization, each cell is characterized every 3 min and 16 s. From the *I–V* characteristics, we extract the short-circuit current, the fill factor, and the maximum power point.

III. RESULTS AND DISCUSSIONS

The test module has been in operation in open-loop tracking mode in the solar park of Université de Sherbrooke from Summer 2021 to Fall 2022. The MCT mode has been implemented in mid-August, 2022. Due to the data filtering, only data acquired until mid-September, 2022, can be used for determining the test module performance, and the module has been dismounted on September 14th, 2022.

Fig. 2(a) presents the evolution of the short-circuit current (I_{SC}) of the four monomodules as a function of the DNI. As expected, we observe a linear variation of the short-circuit current with the DNI for the four monomodules. Based on the measured I_{SC} and the current density (J_{SC}) derived from indoor external quantum efficiency (EQE) measurement before integrating the cells into the module, we can estimate the cell-to-module (CTM) coefficient on the short-circuit current. For this, we calculate the ratio between the measured current at 900 W·m^{-2} and the short-circuit current calculated from EQE measurement, knowing the cell active area (0.0655 cm^2). This ratio gives an effective sun concentration, which should be as close as possible to the lens optical concentration ratio of 250×. The short-circuit current CTM ratio is then defined by the ratio of the effective concentration to 250×. Table I presents the current density derived from EQE, the current measured at the monomodule level for an irradiance of 900 W·m^{-2}, and the effective concentration and the short-circuit current CTM ratio for each monomodule. For all devices except device D, the CTM is between 82% and 90%, which is close to record monomodules presented in the literature [13]. Device D has a CTM of 69%, which will be discussed later. Due to this low performance, we use only device C as a reference

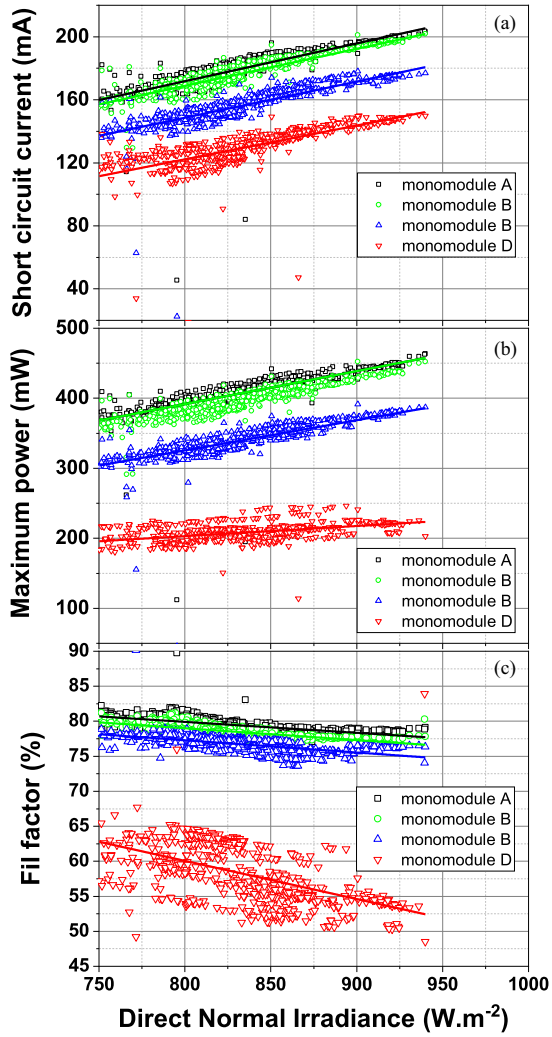

Fig. 2. (a) Short-circuit current, (b) maximum power point, and (c) fill factor as a function of DNI of 250× CPV monomodules after data filtering according to ASTM E2527 method described by the IEC 62670-3 standard (mid-August to mid-September, 2022).

in the following. The CTM losses are attributed to optical losses at the lens (transmission losses through the BK7 glass, reflection losses, comatic aberrations, etc., …), optical losses by reflection of off-normal light on the cell, and to the larger cell temperature. The very high value we measure for the short-circuit current CTM confirms that the cell and tracker alignment procedure enables a quasi-perfect cell/lens/sun alignment.

Monomodules A and B with microbeads encapsulating ARC present a short-circuit current of 196 and 192 mA at 900 W·m^{-2},

and 12%–14% larger than the I_{SC} measured on reference monomodule C (169 mA). This relates also in a larger CTM (89%–90% compared with 82% for the reference). This improvement exceeds the improvement of 2.6% measured in the laboratory condition [8]. This can be explained by a wider angular distribution of the sunlight on the cell into a module compared with indoor conditions. Indeed, the gain of the microbeads ARC compared with interferometric ARC increases when the angle of incidence deviates from the normal of the cell. In addition, the solar spectrum received by the cell into a module may be different from AM1.5D due to absorptions in the lens and due to atmospheric variations, which could enhance the sensitivity to the current of the top or middle junction of the cells. The cell temperature in the module is also larger than in laboratory conditions, which also contributes to increase the short-circuit current when the top cell is limiting the current. Finally, we cannot rule out a faster degradation of the reference cells compared with the microbeads ARC, which would lead to a higher short-circuit current after one year of operation for the cells with microbeads encapsulating ARC. However, preliminary data measured when the module was installed and the tracking mode was in an open loop showed also an improvement of the monomodule with microbeads compared with the article presented in [8].

Fig. 2(b) presents the maximum power produced by the four monomodules as a function of the DNI. As for the short-circuit current, a linear variation of maximum power point (*P*max) as a function of DNI is observed. The maximum power point at 900 W/m^2 is 439 and 425 mW corresponding to a monomodule efficiency of 29.7% and 28.8% for monomodules A and B with microbeads, respectively. This power is 15% to 19% larger than the maximum power measured on reference monomodule C (369 mW, efficiency of 25%). The power and efficiency are reported in Table I.

The improvement in monomodules A and B's performance compared with monomodule C is mostly due to the increase of the short-circuit current, as explained in Section II. An additional improvement is attributed to a larger fill factor (3.7% and 2.4% fill factor increase for monomodules A and B, respectively) since the V_{OC} is almost identical for all three monomodules (2.85 V $\pm$0.01 V). The slightly lower V_{OC} and fill factor of monomodule C can be explained by a different assembly method between reference cells and cells with microbeads encapsulating ARC that may lead to different electrical and thermal resistances. It is, therefore, not attributed to the difference in ARC.

The evolution of the fill factor with the DNI is presented in Fig. 2(c). We can see that the evolution of the fill factor with DNI is similar for monomodules A, B, and C, with a slope of $-1.7.10^{-4}$%/W·m^2 $\pm$0.1%. On the contrary, monomodule D has a dramatically low fill factor (<55% at 900 W/m^2) with a slope of -5.4%/W·m^2. This is indicative of a defective device associated with a strong increase of the series resistance. A visual inspection of cell D (not shown here) when the module was dismounted showed surface residues and degradation of the wire bonding pad that confirm the device's defectivity.

IV. Conclusion

We have integrated solar cells with a graded ARC (microbeads semiburied into a PDMS layer) into a test module and rated the performance of the monomodules after one year in the field. Their performance was compared with monomodules made with reference cells with $AlO_x/TiO_x/SiO_2$ encapsulating ARC. Individual alignment of the solar cells and tracker positioning using MCT enables a quasi-perfect cell/lens/sun alignment. Electrical characterization of the monomodules showed that the solar cells with the microbeads ARC have 12%–14% larger short-circuit current than the reference, exceeding the expectations of 2.6% determined by indoor EQE measurement of the cells. We believe that this improvement comes from the broad angular distribution of light inside the module, compared with normal light incidence during EQE measurements, and from an actual spectrum received by the cell that differs from AM1.5D. A monomodule efficiency of 29.7% and 28.8% is reported for the monomodules with microbeads ARC. This is 3.8%–4.7% absolute better than the reference, mostly explained by a better light collection and to a lower extent by a different cell assembly method.

This article demonstrates, therefore, that integrating a graded ARC, for instance using semiburied silica microbeads in PDMS, enables a significant efficiency gain for CPV modules compared with the conventional multilayer ARC.

References

[1] S. P. Philipps, A. W. Bett, K. Horowitz, and S. Kurtz, *Current Status of Concentrator Photovoltaic (CPV) Technology*. Washington, DC, USA: Office of Energy Efficiency and Renewable Energy, 2015, doi: 10.2172/1351597.

[2] "Solar solutions," STACE commercial brochure, 2022. [Online]. Available: https://www.stacelectric.com/wp-content/uploads/2017/01/STACE-Solar-Solution-Brochure-EN.pdf

[3] D. J. Aiken, "High performance anti-reflection coatings for broadband multi-junction solar cells," *Sol. Energy Mater. Sol. Cells*, vol. 64, pp. 393–404, 2000.

[4] R. Homier et al., "Antireflection coating design for triple-junction III–V/Ge high-efficiency solar cells using low absorption PECVD silicon nitride," *IEEE J. Photovolt.*, vol. 2, no. 3, pp. 393–397, Jul. 2012.

[5] M. Victoria, C. Domínguez, I. Antón, and G. Sala, "Antireflective coatings for multijunction solar cells under wide-angle ray bundles," *Opt. Express*, vol. 20, no. 7, pp. 8136–8147, 2012.

[6] P. García-Linares et al., "Improving optical performance of concentrator cells by means of a deposited nanopattern layer," *AIP Conf. Proc.*, vol. 1679, 2015, Art. no. 040004.

[7] N. Shanmugam, R. Pugazhendhi, R. Madurai Elavarasan, P. Kasiviswanathan, and N. Das, "Anti-reflective coating materials: A holistic review from PV perspective," *Energies*, vol. 13, 2020, Art. no. 2631.

[8] G. P. Forcade et al., "Microstructured antireflective encapsulant on concentrator solar cells," *Prog. Photovolt.: Res. Appl.*, vol. 30, pp. 132–140, 2022.

[9] A. Ritou et al., "CPV module to rate antireflective and encapsulant coating in outdoor conditions," in *AIP Conf. Proc.*, vol. 2550, 2022, Art. no. 030004.

[10] Thorlabs web site, 2022. [Online]. Available: https://www.thorlabs.com/newgrouppage9.cfm?objectgroup_id=112&pn=LA1145

[11] Eko website, 2022. [Online]. Available: https://www.eko-instruments.com/eu/categories/products/sun-trackers/str-22g-sun-tracker

[12] M. Muller, "Minimizing variation in outdoor CPV power ratings," in *Proc. Rel. Workshop*, Golden CO, USA, 2011, pp. 336–340.

[13] M. Steiner et al., "FLATCON CPV module with 36.7% efficiency equipped with four-junction solar cells," *Prog. Photovolt.: Res. Appl.*, vol. 23, pp. 1323–1329, 2015.